DINAME 2017 - Proceedings of the XVII International Symposium on Dynamic Problems of Mechanics
A.T. Fleury, D. A. Rade, P. R. G. Kurka (Editors), ABCM, São Sebastião, SP, Brazil, March 5-10, 2017

TUNABLE AUXILIARY MASS DAMPER WITH FRICTION JOINT: NUMERICAL ASSESSMENT AND PROTOTYPE DESIGN

H.T. Coelho[1], **F.P. Lepore Neto**[1], **M.B. Santos**[1]

[1] Laboratory of Mechanical Systems, Mechanical Engineering School, Federal University of Uberlandia, Brazil. Avenida Joao Naves de Avila, 2121 - Campus Santa Monica, Bolco 1M, Terreo – Uberlandia - Minas Gerais – Brazil – Zip Code: 38400-902; humberto.tc@ufu.br; fplepore@mecanica.ufu.br; marcelo.bragadossantos@ufu.br

Abstract: Auxiliary Mass Dampers (AMD) are often used to reduce excessive vibration amplitude in mechanical systems, it is also known that their performances are susceptible to changes in the frequency or in the excitation force's nature (impulsive, transient, random, periodic). Therefore, to improve the robustness of the AMD it is necessary to design new systems which are adaptable to the excitation, i.e., tunable devices that could be used over large frequency range. In this work a friction damper, which is association in series of a spring and a scratcher, is used to tune the AMD by changing the normal force on the scratcher, at the same time it dissipates the mechanical energy of the principal mass, this AMD is namely Tunable Auxiliary Mass Damper (TAMD). Three normal force control strategies, and two combinations of them, are studied: i) The normal force is assumed constant; ii) The normal force is obtained from the solution of the equation of motion assuming null displacement for the principal mass; iii) The normal force is obtained based on the vibratory system's movement, guarantying that the direction of the friction force promotes the movement of the principal mass toward its static equilibrium position. The effectiveness of the proposed TAMD is evaluated based on mass and frequency ratios variations for each strategy. Therefore, the goal is to design a TAMD prototype that meets the design requirements presented in this work and allows obtaining in future work experimental results that proves the device efficiency.

Keywords: Tunable Auxiliary Mass Damper, Variable Damped Absorber, Semi-Active Device Control Strategies, Design of Vibration Attenuation Device and Friction Damper

INTRODUCTION

Auxiliary masses are frequently attached to vibrating systems by springs and damping devices aiming to reduce the excessive vibration amplitude. Depending on the application, these auxiliary mass systems fall into one of two distinct classes. A Dynamic Vibration Absorber (DVA) is an auxiliary mass on a compliant suspension, which has a damping factor as lower as possible, once it is tuned on the frequency of the excitation force a system's antiresonance is introduced reducing the primary system's vibration amplitudes. If necessary to provide damping, an auxiliary system with viscous damping is attached to the structure, so that, the auxiliary mass system works as a particular type of damper. It is called Damped Absorber or Auxiliary Mass Damper (AMD) being an extension of the DVA concept (Harris and Piersol, 2002).

To improve the AMD's performance on the vibration attenuation some researchers use an active device on its suspension. These devices are active springs, made with memory shape alloys, piezo stacks and other actuators able to tune the AMD on a desired frequency (Chatterjee, 2010). Other solutions are the semi-active systems, which use friction dampers (Lu *et al*, 2006 and Lin *et a*l, 2010) or magnetorheological dampers (Weber, 2014) to tune the frequency of the AMD system and simultaneously dissipate the mechanical energy.

AMD enables to reduce vibration amplitudes without energy consumption, within a narrow frequency band for which the AMD has been tuned. Unfortunately, when changes in the excitation nature or in the system parameters occur, its performance drops drastically. To improve AMD's robustness a suitable approach is a semi-active absorber (or adaptive, tunable), which changes its characteristics according the necessities. Such a device has its physical parameters, as consequence also its impedance, adjustable. Associated to a suitable control law it is possible to adapt the system to different variety of excitations reducing the vibration amplitude. In this way, the system becomes a Tunable Auxiliary Mass Damper (TAMD).

The energy necessary to tune the AMD is much less than the energy necessary to achieve the same attenuation using active actuators, once for the active systems the energy is expended to work against the excitation force.

The aim of this work is to develop a new TAMD where the adaptability is obtained by controlling the normal force of a smart friction damper. The numerical study demonstrates the effectiveness of the developed strategy and indicates the mass and frequency ratios to be used on the design of the TAMD prototype that will allow, in future work, obtain experimental results to confirm the device efficiency calculated using numerical simulations.

THEORETICAL APPROACH

The TAMD has been applied to a one Degree of Freedom (DOF) vibratory system as shown on Coelho *et al* (2016) and Guerineau *et al* (2016), the schema of the system studied is shown on Fig.1a. It is a two DOFs that can be modeled as a one DOF linear vibratory system (m_1, in black) coupled to an AMD using a friction damper (m_2, in red).

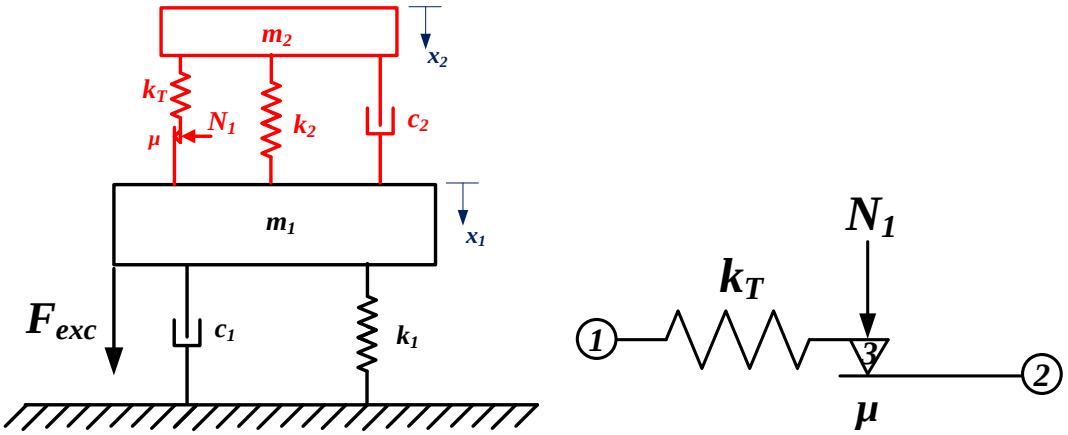

Figure 1 – (a) Schema of the system studied and (b) Friction damper model.

The adaptability is achieved using a friction damper (Fig. 1b). It is association in series of a spring and a scratcher which will tune the TAMD. This system enables to dissipate the mechanical energy of the principal mass, by changing the normal force on the scratcher, therefore the apparent damping coefficient and stiffness of the TAMD's suspension are changed. The force between nodes (1) and (2), indicated on Fig. 1b, is F_{12} and can be written as presented on Eq.(1).

$$F_{12} = \begin{cases} k_T(x_2 - x_1) & if \quad k_T(x_2 - x_1) \leq \mu N_1 \\ \mu N_1 & if \quad k_T(x_2 - x_1) > \mu N_1 \end{cases} \tag{1}$$

Points (1) and (2) from friction damper, as shown on Fig. 1b, are attached to mass m_1 and m_2 of the vibratory system respectively. The TAMD's suspension is composed by the stiffness k_2 and the damping c_2, as linear elements, and the nonlinear component characterized by the tangential stiffness k_T and the scratcher which has its force as defined in Eq.(1). The suspension between m_1 and the inertial frame is composed by the stiffness k_1 and the damping c_1. The motion equation for the entire system becomes:

$$\begin{bmatrix} m_1 & 0 \\ 0 & m_2 \end{bmatrix} \begin{Bmatrix} \ddot{x}_1 \\ \ddot{x}_2 \end{Bmatrix} + \begin{bmatrix} c_1 + c_2 & -c_2 \\ -c_2 & c_2 \end{bmatrix} \begin{Bmatrix} \dot{x}_1 \\ \dot{x}_2 \end{Bmatrix} + \begin{bmatrix} k_1 + k_2 & -k_2 \\ -k_2 & k_2 \end{bmatrix} \begin{Bmatrix} x_1 \\ x_2 \end{Bmatrix} = \begin{bmatrix} 1 \\ -1 \end{bmatrix} F_{12} + \begin{bmatrix} 1 \\ 0 \end{bmatrix} F_{exc} \tag{2}$$

The equation of motion has been integrated using the methodology proposed by Lu *et al* (2006) which, uses the state space formulation from the linear system, and dispose the nonlinear force from friction damper as part of the excitation forces.

Knowing that mass (m_2/m_1) and frequency (ω_2/ω_1) ratios affect DVA's and AMD's behavior, the numerical assessment aimed to determine the best ones to be used for the future experimental workbench, under design. As mentioned before TAMD works associated to a control law. Five control laws are used in an attempt to minimize the vibration amplitude of the principal mass by directing the energy to the TAMD and use the relative displacement promoted in the friction damper to dissipate the mechanical energy. All control laws aims to produce an efficient energy sink. There are three main normal force control strategies, and two combinations of them: i) The normal force is assumed constant [S1]; ii) The normal force is obtained, from Eq.(3), which is the solution of the equation of motion assuming null displacement for the principal mass, i.e. $x_1 = 0$ [S2]; iii) When F_{12} induces a movement of m_1 towards its static equilibrium position the normal force is stemming from Eq.(4), otherwise it is null [S3]. The strategy [S4] uses the same logic described for [S3], but now the normal force is calculated using Eq.(3). And [S5] also uses the logic developed for [S3], however as for [S1] it uses a constant value for the normal force N_1.

$$N_1 = \frac{|m_2\ddot{x}_2 + c_2\dot{x}_2 + k_2x_2|}{\mu} \tag{3}$$

$$N_1 = \frac{k_T(x_2 - x_1)}{\mu} \tag{4}$$

To compare all control methodologies it is necessary to establish a criterion that enables to show the reduction of the resonance amplitude peak simultaneously to the reduction of the amplitude of the receptance over the entire interested frequency band. It is clear from the literature that DVA split the original resonant peak in two new resonant peaks, which, can be disastrous to the vibratory system if the excitation force contains harmonics with these new resonant frequencies. Normally, two parameters are used simultaneously to describe the performance of the control systems: Maximum Value ($L_\infty\ norm$) and the $L_2\ norm$. The former indicates the maximum amplitude expected for the system response and the second the overall mean value of the response. A similar statement has been used in the control technique H_∞/H_2 (Rotea and Khargonekar, 1991). Therefore, in this work the performance parameter (P_p) is defined as the ratio $(L_\infty\ norm)/(L_2\ norm)$ where the best control law performance will provide the lowest values for both norms. In this work the performance parameter (P_p) is defined as:

$$P_p = \frac{maximum\ receptance\ amplitude}{receptance\ amplitude\ norm} \tag{5}$$

Assuming a column vector $A = [\varepsilon\ \varepsilon\ \varepsilon\ ...\ A_1\ ...\ \varepsilon\ \varepsilon\ \varepsilon]_{1xN}$, where ε is a real constant closest to zero and A_1 a real positive constant, which represents the receptance with one peak only on the frequency spectrum $A = A_1\delta(f_1)$, where $\delta(f_1)$ is the Dirac function on the frequency f_1, the parameter P_p can be written as:

$$P_p = \lim_{\varepsilon\to 0} P_p = \lim_{\varepsilon\to 0} \frac{A_1}{\sqrt{(N-1)\varepsilon^2 + A_1^2}} = \frac{A_1}{A_1} = 1 \tag{6}$$

The other extreme is a constant amplitude receptance, which are represented by the column vector $A = [\varepsilon\ \varepsilon\ \varepsilon\ ...\ \varepsilon\ \varepsilon\ \varepsilon]_{1xN}$ for this the parameter P_p is written as:

$$P_p = \lim_{\varepsilon\to 0} P_p = \lim_{\varepsilon\to 0} \frac{\varepsilon}{\sqrt{N\varepsilon^2}} = \frac{1}{\sqrt{N}} \tag{7}$$

Equations (6) and (7) give the maximum and minimum values of the performance parameter as defined on Eq. (5).

NUMERICAL RESULTS

To obtain a reasonable comparison among the obtained results and those of the literature, mass and frequency ratios are the same described by Harris and Piersol (2002). The effectiveness of the proposed TAMD, where the adaptability is obtained by controlling the normal force on the smart friction damper, is evaluated based on mass and frequency ratios variations for each strategy. In this work the mass ratios studied are $m_2/m_1 = [0.1, 0.2, 0.3, 0.4, 0.5]$ and for the frequency are $\omega_2/\omega_1 = [0.1, 0.5, 1]$. These ratios with the five control strategies are compared to the correspondent optimum viscous damping AMD, to a well-tuned DVA and to the 1 DOF free vibration response.

The numerical results presented at this section has been obtained using the following physical parameters values, which represent the parameters from a designed modification of the experimental workbench used on previously works (Guerineau *et al*, 2016 and Coelho *et a*l, 2016), $m_1 = 4.14\ kg$, $c_1 = 3.93\ Ns/m$ and $k_1 = 70.3k\ N/m$. The physical parameters for the secondary system (m_2, c_2 and k_2) are deduced from the mass and frequency ratios aforementioned. The contact parameters are the tangential stiffness $k_T = 5.115x10^5\ N/m$ and the friction coefficient $\mu = 0.1689$. These parameters are theoretical ones, obtained based o contact pair characteristics, and should be estimated as soon as the test rig has been constructed.

All receptances had been obtained using an harmonic force excitation with an amplitude of $10N$. The excitation force frequency has been swept from $5\ Hz$ up to $100\ Hz$, in steps of $1\ Hz$. It was assumed that the stead state response was obtained after 60 periods of oscillation, and the successive 30 periods has been used to estimate the cross and auto spectrum functions. These parameters have been chosen after an observation of the system response at the resonance. For strategies which use constant normal force value, $N_1 = 20N$ has been applied. Again these values come from previous tests, which also had determined that the ratio $N_1/F_{exc} = 2$ is the best to be used for constant normal force (Guerineau *et al*, 2016 and Coelho *et a*l, 2016).

The values of the performance parameter P_p for all combinations of control strategies, mass and frequency ratios are shown on Figure 2. Additionally, for comparison the performance parameter for 1 DOF free vibration system, the vibratory system coupled to AMD with optimum viscous damping and the system coupled to a well-tuned DVA are also shown on Figure 2. The best responses are the ones that has the lowest norm and the lowest peak value, i.e., are located in the lower left corner in the figure. Should be clear that P_p is a parameter to give a metric for optimization procedures, it can't be used as a substitute for the receptance analysis where it is possible to see how much the solution is closest of the optimum, i.e., how much it is closest to the lowest norm and the lowest peak of resonance which aim the engineers. On Figure 2 the color bar indicates the value of P_p and the arrows indicate the location of the best result

for each control strategy, also for the location of the DVA, optimum viscous damping AMD and the 1DOF free vibration. The last one refers to the system composed only by m_1, k_1 and c_1.

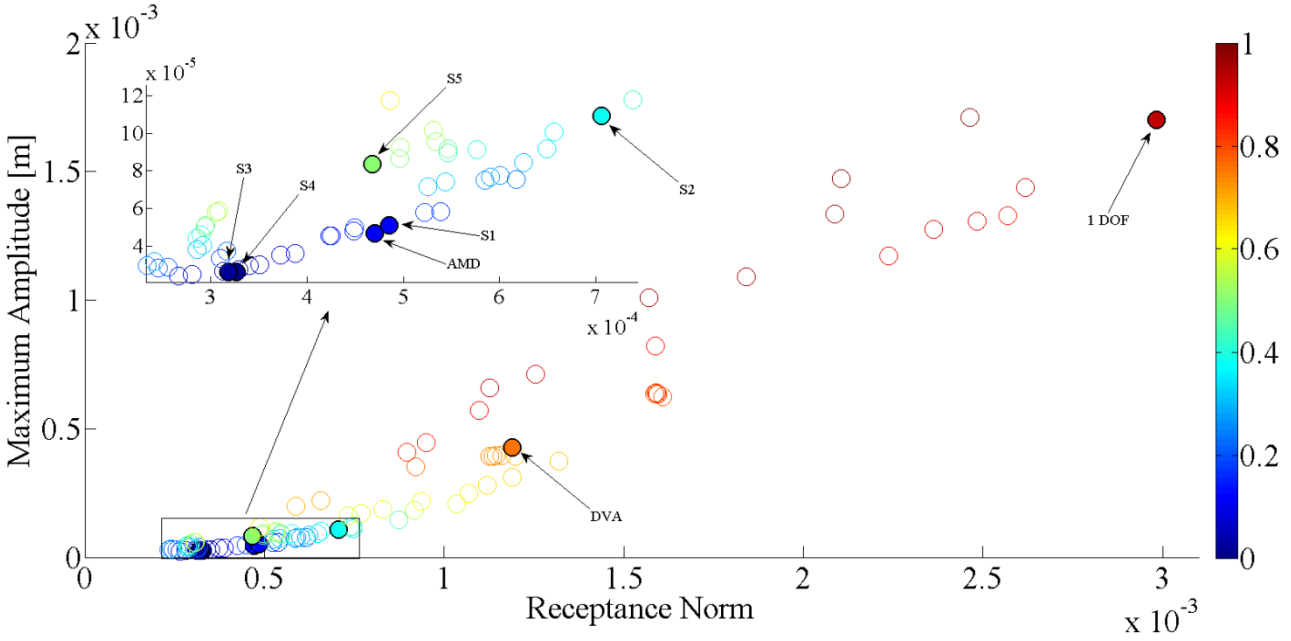

Figure 2 – Maximum amplitude and receptance norm chart.

On the Figure 3 are presented the best response for each control strategy and compares them with the best optimum viscous damping AMD result, the well-tuned DVA and the 1 DOF free vibration response.

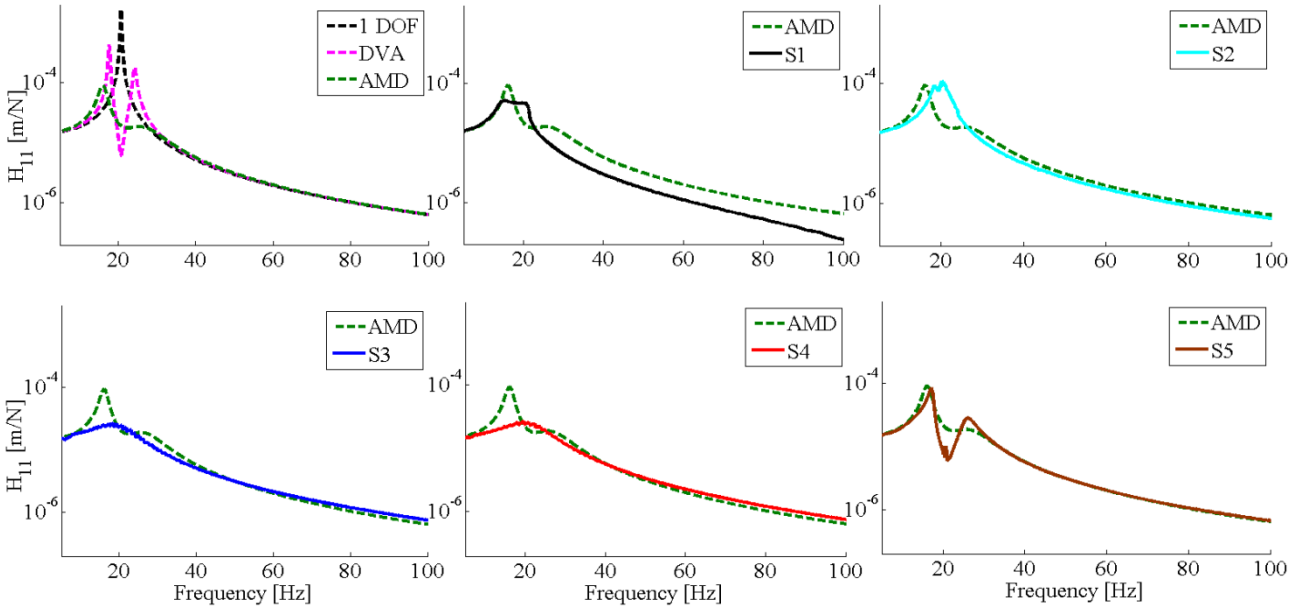

Figure 3 – Receptance results for the best of each strategy.

The best receptances are for [S3] and [S4], they present, at the same time, the lowest peaks and the lowest norm. Based on these receptance results, it can be conclude that the proposed semi-active suspension almost entirely suppressed the resonance peaks. Should be also observed that the receptances for [S3] and [S4] had almost their entirely values at the same levels or lower than the static response, which is a great advantage for the proposed TAMD. These results demonstrate that the TAMD can be effective in a wide frequency range once that all strategies promote an improvement in the attenuation of the resonant peaks as well as in the L_2 $norm$ value. They are also promoting a better response than that obtained by optimal viscous damped AMD. Strategies [S1], [S2] and [S5] also present good receptances, almost as good as the optimum damping AMD, their highest values for P_p are due the maximum amplitude of the receptance which are a little higher than [S3] and [S4] maximum amplitude. It should be noticed that all strategies give better results than well-tuned DVA.

Table 1 summarizes the mass and frequency ratios combination on which was obtained the lowest values for P_p for each strategy. Also presents the ratios used to tune the DVA, those that has presented the best optimum viscous damping AMD response and their respective performance parameter value. The 1 DOF free vibration have also had its receptance quantified by using the performance parameter P_p.

Table 1 – Ratios combination and P_p value for the bests of each strategy.

CONTROL STRATEGY	RATIOS COMBINATION		P_p
	ω_2/ω_1	m_2/m_1	
1 DOF	$(-)$	$(-)$	0.570
DVA	1.0	0.1	0.359
AMD	0.5	0.5	0.099
STRATEGY S1	0.5	0.5	0.105
STRATEGY S2	1.0	0.1	0.154
STRATEGY S3	0.1	0.5	0.083
STRATEGY S4	0.1	0.5	0.081
STRATEGY S5	1.0	0.1	0.178

As observed strategies [S3] and [S4] has presented excellent results, however with mass ratio $m_2/m_1 = 0.5$, which is too much mass to be added. Strategies [S2] and [S5] have their best performance for mass ratio $m_2/m_1 = 0.1$ and frequency ratio $\omega_2/\omega_1 = 1$. So for this ratio combination the P_p values for the optimum viscous damping AMD, [S1], [S3] and [S4] was 0.153, 0.166, 0.109 and 0.119 respectively, which are excellent values when compared to the mass reduction that was possible to achieved. Note that strategies [S3] and [S4] performance parameter values remains smaller than for [S2] and [S5] presented on Tab. 1. Here becomes clear a compromise solution between the mass ratio and the performance parameter. Changing the mass ratio for 10% and recalculating again the receptances is possible to verify that strategies [S3] and [S4] remains the better ones as shown on Fig. 4.

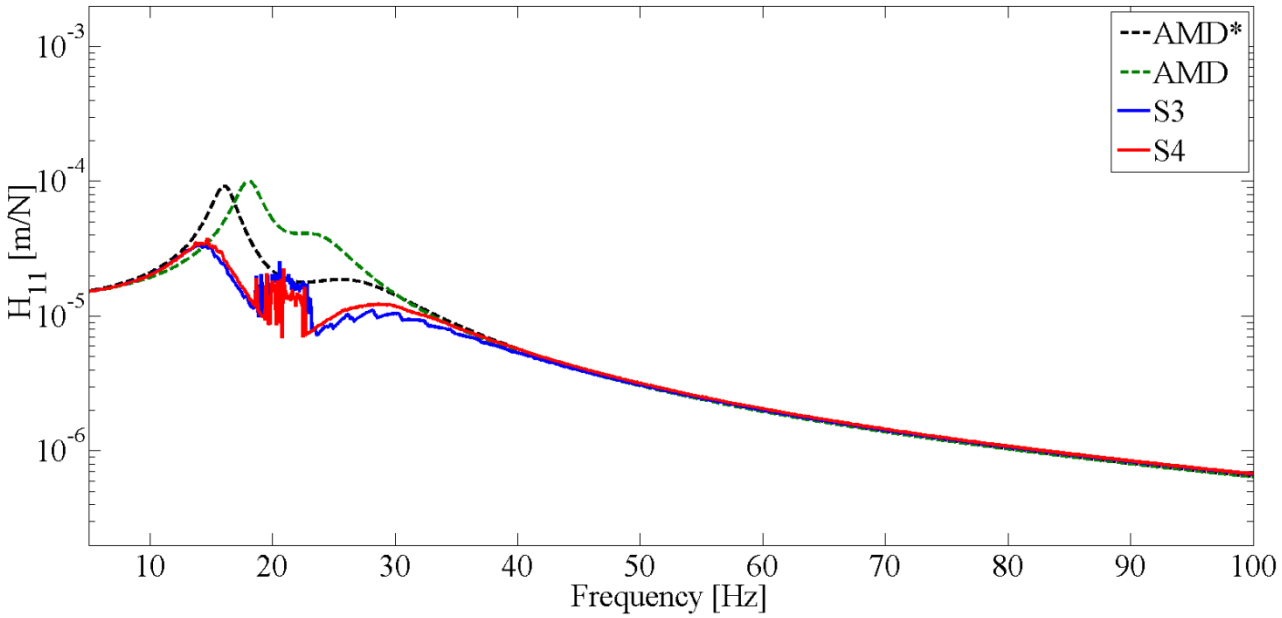

Figure 4 – Receptance results for $m_2/m_1 = 0.1$ and $\omega_2/\omega_1 = 1$. Optimum viscous damping AMD response with a mass ratio $m_2/m_1 = 0.5$ (AMD*), optimum viscous damping AMD response (AMD), TAMD response using strategy S3 (S3) and TAMD response using strategy S4 (S4).

The symbol $(*)$ at the legend indicates the optimum viscous damping AMD receptance previously obtained with a mass ratio $m_2/m_1 = 0.5$. Besides the good aspect of the receptances, presented on the Fig. 4, they are little worse than ones presented on Fig.3. Concerning the compromise solution between the mass ratio and the performance of the proposed TAMD, the worsening of the receptances are justified by the great reduction on the mass to be added on the system. Besides, strategies [S3] and [S4] receptance remains better than optimum viscous damping AMD in almost one order of magnitude attenuation for the receptance maximum value on the chosen ratios.

To evaluate the robustness of the TAMD with the chosen mass and frequency ratios it was also performed a numerical study with other types of excitation force (which not the harmonic use to obtain the receptances) for

strategies [S3] and [S4] which are clearly better than the others. Figure 5 presents the system's time response of m_1 displacement to an 10 N impact excitation applied at 0.5 s to the 2 DOF presented on Fig. 1a.

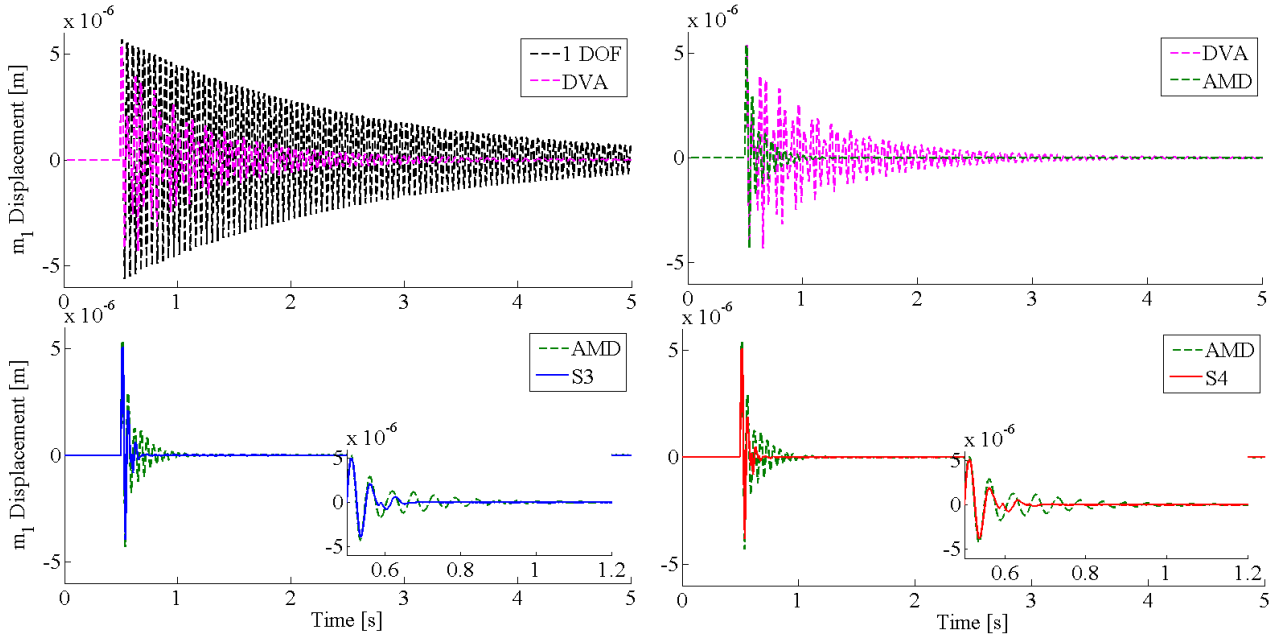

Figure 5 – Time response to an impact excitation for $m_2/m_1 = 0.1$ and $\omega_2/\omega_1 = 1$. Free vibration response of without auxiliary mass (1 DOF), well-tuned DVA response (DVA), optimum viscous damping AMD response (AMD), TAMD response using strategy S3 (S3) and TAMD response using strategy S4 (S4).

It can be noted that strategies [S3] and [S4] presents the lowest settling time showing an excellent damping capability. They had better responses than optimum viscous damping AMD, which in turn is better than DVA's response. Figure 6 presents the time response to a random excitation.

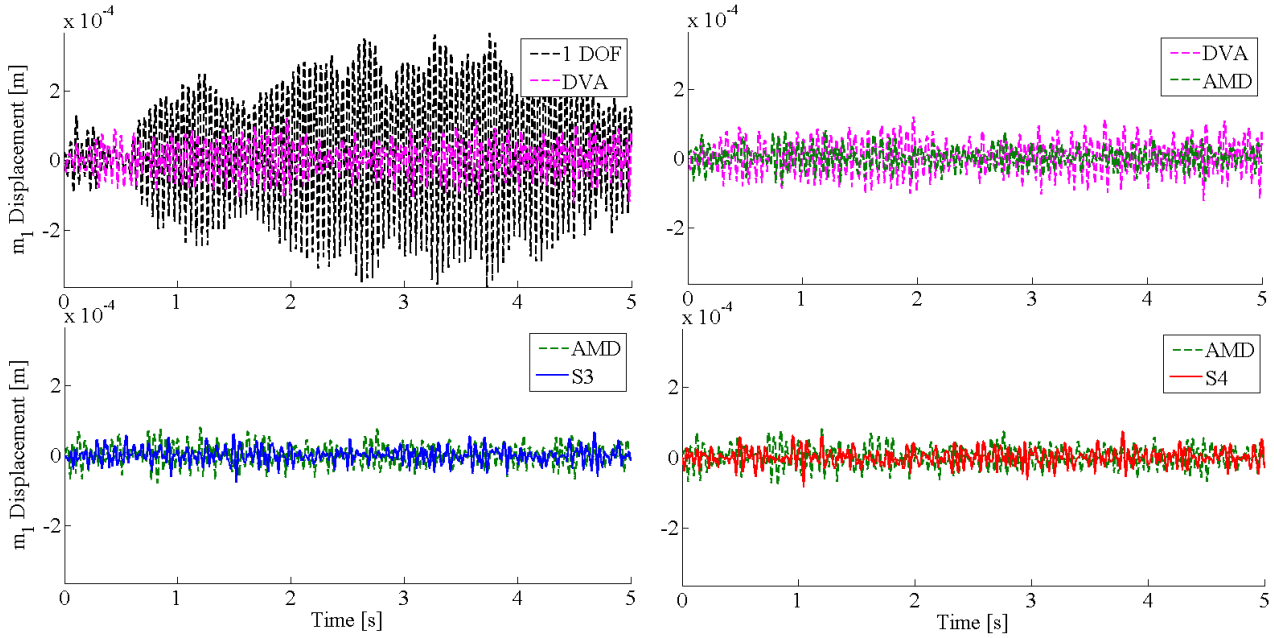

Figure 6 – Time response to a random excitation for $m_2/m_1 = 0.1$ and $\omega_2/\omega_1 = 1$. Free vibration response of without auxiliary mass (1 DOF), well-tuned DVA response (DVA), optimum viscous damping AMD response (AMD), TAMD response using strategy S3 (S3) and TAMD response using strategy S4 (S4).

Normally is too difficult to deal with random excitations due its nature, especially for semi-active systems, which try to tune the vibratory system to the excitation force, maximizing the performance of the TAMD. It can be noted that DVA's presents a better response than 1 DOF system's free vibration, with RMS amplitude of 45.1 μm and 162.2 μm respectively. A good improvement is obtained with optimal viscous damped AMD response with RMS amplitude of 27.2 μm and responses even better can be observed for the results obtained with [S3] and [S4]. The RMS values for

these responses are 19.8 μm and 21.2 μm, respectively for [S3] and [S4], which are less than half of the DVA's RMS and eight times smaller than 1 DOF system's free vibration RMS.

The time response of each strategy and DVA for chirp excitation with its frequency sweeping from 5 Hz up to 100 Hz, changing in a ratio of 19 Hz/s, are presented on Fig. 7.

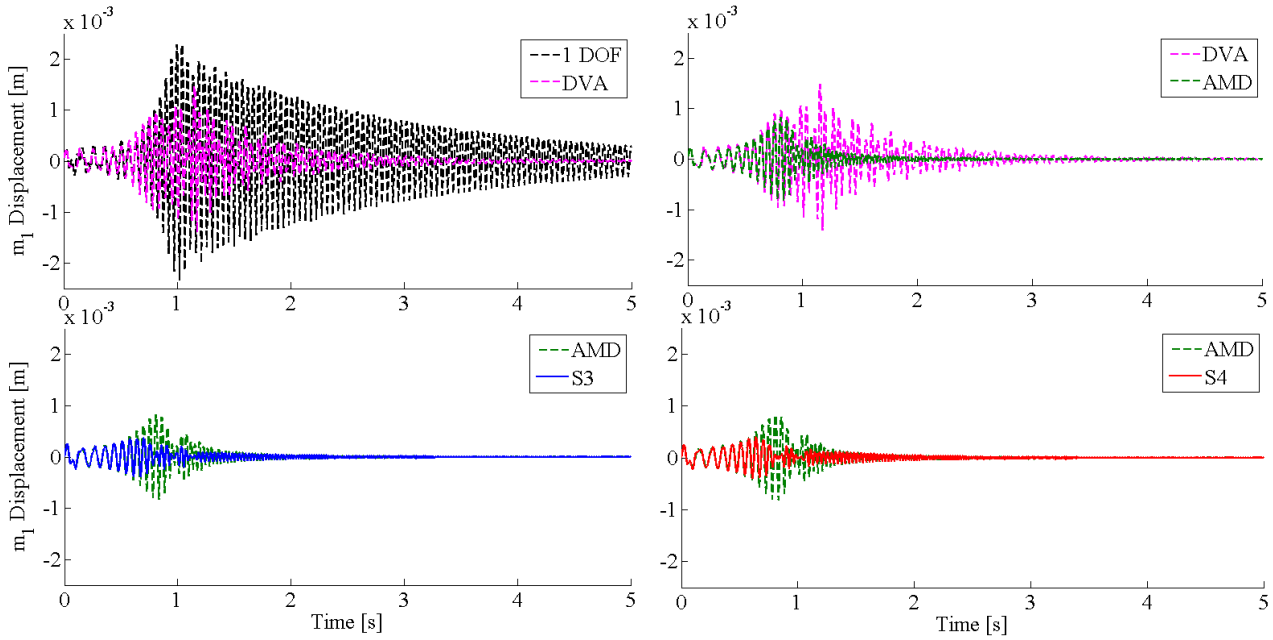

Figure 7 – Time response to a chirp excitation for $m_2/m_1 = 0.1$ and $\omega_2/\omega_1 = 1$. Free vibration response of without auxiliary mass (1 DOF), well-tuned DVA response (DVA), optimum viscous damping AMD response (AMD), TAMD response using strategy S3 (S3) and TAMD response using strategy S4 (S4).

The 1 DOF response presents a maximum amplitude of 2.28 mm near 1.0 s, which is bigger than DVA's response with 1.48 mm around 1.5 s. The optimal viscous damped AMD maximum amplitude is 0.82 mm. The strategies [S3] and [S4] presents better results than AMD's response with the lowest amplitudes, in which the passage through resonance is almost imperceptible, with maximum amplitudes of 0.37 mm and 0.39 mm respectively. This last fact could be useful for applications on rotating machines permitting a smoother passage through critical speeds.

Therefore, in this numerical study of the TAMD was also verified that the proposed control strategies' efficiencies are independent of the excitation force nature and that strategies [S3] and [S4] presents better results than optimal viscous damped AMD, which is nowadays some of the best design alternatives for vibration attenuation.

PROTOTYPE DESIGN

The good results obtained in the numerical assessment of the TAMD leads to the design of a test rig that should be able to experimentally verify these results, to be done in the future. On this numerical assessment has been determined the best mass and frequency ratios, which are used to determine the TAMD's physical properties based on mass and frequency of an already existing 1 DOF experimental workbench.

The TAMD's design characteristics are:

a) The TAMD to be designed must couple at a 1 DOF experimental workbench already existing shown on Fig. 8.

b) The TAMD should have its DOF oriented with the DOF of the experimental workbench as shown on Fig. 8.

c) The structure of the TAMD responsible to fix it on the experimental workbench must be as light as possible, but with sufficient stiffness to effective transmit the forces between the TAMD and the workbench.

d) The workbench to be designed must present a symmetrical force application system, and it shall not introduce any torque in the auxiliary mass that may be able to change the direction of its movement.

e) The friction coupling, on the TAMD's suspension, shall allow non-contact situations.

f) The chosen actuator is a Cedrat® APA 500L piezoelectric stack, with its maximum load capacity of 607 N and promoting a 517 μm maximum displacement.

g) A tri-axial load cell model ATI® Mini45 makes possible the measurement of the normal force magnitude and the friction force in the contact as well.

h) The TAMD must allow a 5 mm relative displacement between masses m_1 and m_2 to allow the correct functioning of the device without the collision between the auxiliary mass and the frame that fixes and supports it.

A schematic diagram of the TAMD operation is shown on Fig. 9 and further the mechanical design on Fig. 10.

By means of the linear suspension, composed by eight parallels beams, is designed to be very flexible in the desired movement direction and almost perfectly rigid on the others 5 DOF has been assured that the auxiliary mass has only 1 DOF within the studied frequency band. The length of the flexure beams also guarantees that they present a linear behavior in the displacement range that was estimated on the numerical models. The parallels beams (linear suspension) and the auxiliary spring, shown on Fig. 9, compose the stiffness k_2 of the model shown on Fig. 1a.

To attend the requirement c) it was decided to use aluminum alloys in the frame's manufacture. Figure 10 presents the project design.

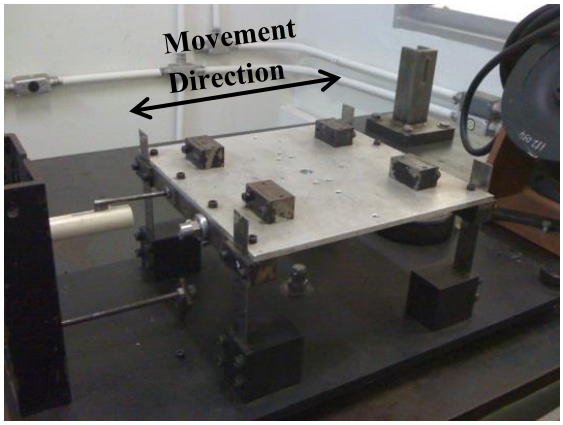

Figure 8 – Experimental workbench already existing – Part of the principal vibratory system.

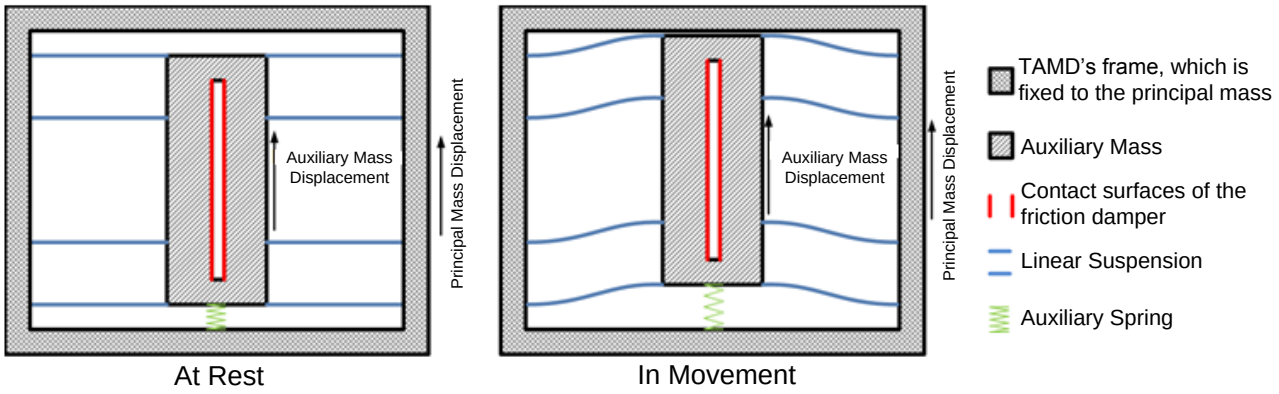

Figure 9 – Schematic diagram of the frame that fixes and supports the auxiliary mass of the proposed TAMD.

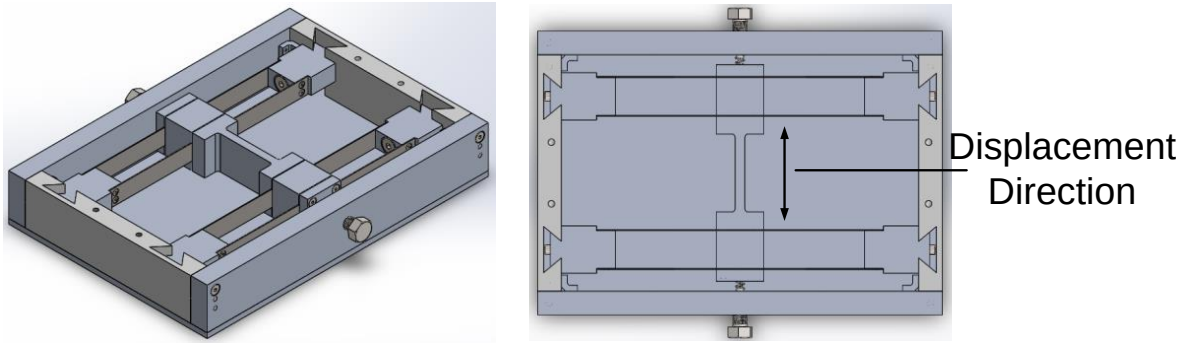

Figure 10 – Frame that fixes and supports the auxiliary mass of the proposed TAMD.

The normal force is applied by using a floating caliper, assuring that is symmetrically applied on the contact surfaces shown on Fig. 9. This is a design exigence placed on item d). This floating caliper is fixed to the frame by linear guide bearings, which can be seen in details on Fig. 11. Therefore, all assembly, except the auxiliary mass m_2, will have the same displacement that the principal mass, i.e., the floating caliper, the frame and the supporting bearing are also part of the principal mass m_1. These masses are added to the moving mass of the workbench shown on the Fig.8, which all of them compose the mass m_1 of the model shown on the Fig. 1a. Another interesting factor in the use of a floating caliper is that it can perform clearance compensation by itself. The choice for a floating caliper also allows to meet the requirement e).

The support of the actuator Cedrat® APA 500L piezoelectric stack is designed to be very rigid and as light as possible aiming maximize the amplitude of the applied normal force and minimize the settle time.

The floating caliper is guided by SKF® LQCR-8 linear bearings. The chosen tri-axial load cell measures simultaneously the normal and the friction force. The resultant friction force, which is the sum of the forces in both contact surfaces, is measured by the load cell just on its side, then it is necessary to multiple its value by two on the control methodology. Spheres are used as counter bodies to apply the normal force on the contact surfaces of the auxiliary mass shown in red on Fig. 9.

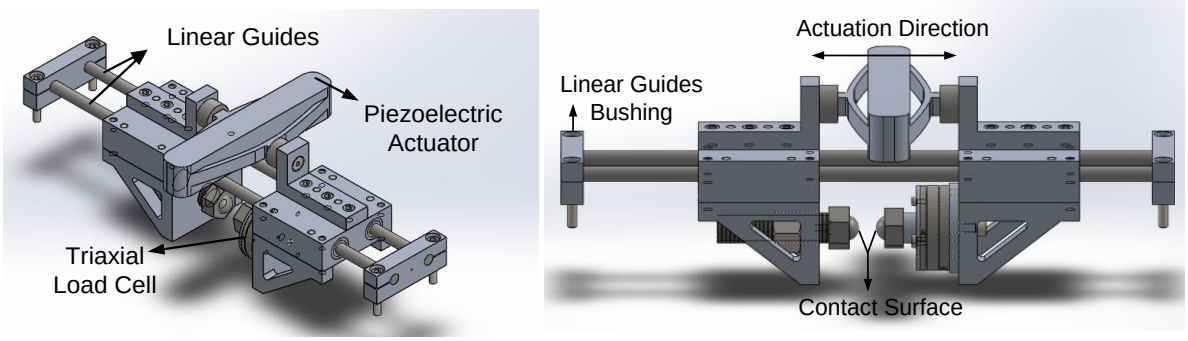

Figure 11 – Floating caliper views of the proposed TAMD.

Figure 12 presents a general view of the TAMD prototype assembly , which can be clearly noted that is the assembly of both parts of the design project, the floating caliper (Fig. 11ab) and the frame that fixes and supports the auxiliary mass of the proposed TAMD (Fig. 10).

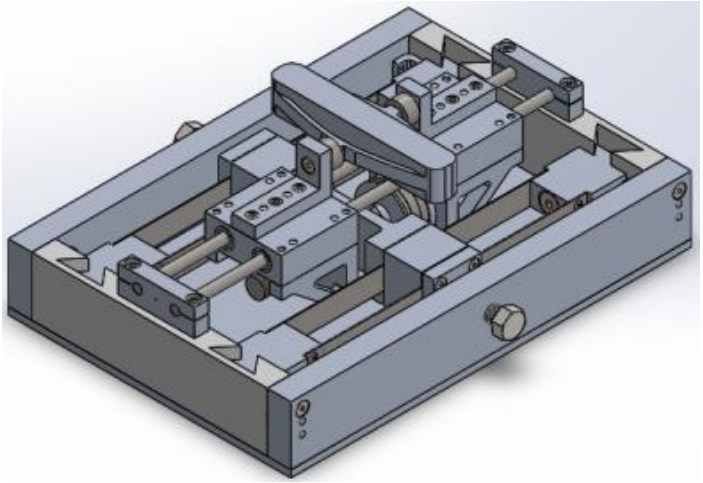

Figure 12 – View of the assembly of the TAMD prototype.

CONCLUSIONS

A performance parameter has been defined and was shown to be effective as a metric for optimization procedures, identifying the receptance with the lowest peak and the lowest $L_2\ norm$ over the analyzed frequency band. Through the presented numerical simulations is possible to affirm that the proposed TAMD model presents better results than the traditional DVA.

TAMD's selected strategies are capable to achieve excellent performance, with low mass ratios, for different kind of excitation and present results even better than optimal viscous damped AMD, which is nowadays some of the best design alternatives for vibration attenuation. Those results certify the TAMD as able to be used in a wide range of applications, and the fact that requires only a 10% mass addition it can be used on embedded systems with weight restriction.

Likewise, the fact that it makes use of friction dampers it is also allow it to be used with heavy and big structures applications even under low velocities of vibration were viscous dampers are inefficient or unfeasible due its size.

The design's requirements were stablished and the prototype final design is considered satisfactory. Efforts were made to get as less mass as possible, to attend symmetry and sufficient stiffness condition as well, to permit movement in only one direction in the frequency range to be analyzed. Thus the prototype design is considered ready to be made and compose the experimental workbench aiming to obtain results that proves the proposed device efficiency.

ACKNOWLEDGEMENTS

The authors are grateful to the agencies and bureaus which had been supported this research project: Capes, Fapemig and CNPq.

REFERENCES

Chatterjee, S., Optimal active absorber with internal state feedback for controlling resonant and transient vibration, Journal of Sound and Vibration, 329, p. 5397–5414, 2010.

Coelho, H.T., Lepore Neto, F.P. e Santos, M.B. Numerical Assessment of a Tunable Auxiliary Mass Damper Using a Friction Damper. Society for Experimental Mechanics – IMAC-XXXIV - Dynamics of Multiphysical Systems: From Active Materials to Vibroacoustics, 2016.

Guerineau, E.L.C., Coelho, H.T., Lepore Neto, F.P., Santos, M.B. e Mahfoud, J. On the Assessment of a Tunable Auxiliary Mass Damper with a Friction Damper in its Suspension: Numerical Study. Third International Conference on Structural Nonlinear Dynamics and Diagnosis – CSNDD, 2016.

Harris, C.M., Piersol, A.G. Harris' Shock and Vibration Handbook. Fifth Edition. McGraw-Hill HANDBOOKS, 2002.

Lu, L.-Y.; Chung, L.-L.; Wu, L.Y. and Lin, G.-L. Dynamic Analysis of Structures with Friction Devices Using Discrete-Time State-Space Formulation. Computers and Structures. Taiwan, v. 84, p. 1049-1071, 2006.

Lin, C.-C, Lin, G.-L. and Wang, J.-F., Protection of seismic structures using semi-active friction TDM, Earthquake Engineering and Structural Dynamics, 39, p. 635–659, 2010.

Rotea, M.A. and Khargonekar, P.P., Mixed H^2-optimal Control with an H^∞-constraint: The State Feedback Case, Automatica, 27(2): p. 307-316, 1991.

Weber, F., Semi-active vibration absorber based on real-time controlled MR damper, Mechanical Systems and Signal Processing, 46, p. 272–288, 2014.6.

RESPONSIBILITY NOTICE

The author(s) is (are) the only responsible for the material included in this paper.